Available online at www.sciencedirect.com

SCIENCE DIRECT®

Journal of Steroid Biochemistry & Molecular Biology 92 (2004) 419–433

The Journal of Steroid Biochemistry & Molecular Biology

www.elsevier.com/locate/jsbmb

Requirements for reliable determination of binding affinity constants by saturation analysis approach

Jean-Louis Borgna*

INSERM U. 540, 60 rue de Navacelles, 34090 Montpellier, France

Received 27 May 2004; accepted 25 August 2004

Abstract

Accurate calculation of the equilibrium association constant (K) and binding site concentration (N) related to a receptor (R)/ligand (L) interaction, via R saturation analysis, requires exact determination of the specifically bound L concentration (B_S) and the unbound L concentration (U) at equilibrium. However, most binding determinations involve a procedure for separation of bound and unbound L. In such situations, it was previously shown that correct calculation of B_S and U from binding data requires prior determination of α, i.e. the procedure parameter representing the proportion of equilibrium B_S recovered after running the separation process, and of kn, i.e. the equilibrium nonspecific binding coefficient. For the simplest model of R/L interaction, the consequences of α neglect and/or kn neglect on determination of K and N, via R saturation analysis, are investigated. When α but not kn has been determined, B_S can be accurately calculated, whereas U is overestimated by factor ($kn + 1$). Consequently the type (linear or hyperbolic) of theoretic curves obtained by usual representations (such as the Scatchard, the Lineweaver–Burk or the Michaelis–Menten plot) of the R/L binding is unchanged; these curves afford correct N and underestimation of K by factor ($kn + 1$). When α ($\alpha < 1$) has not been determined B_S and U are underestimated and overestimated, respectively. Then erroneous representations of the R/L binding result (e.g. instead of regular straight line segments, Scatchard plot and Lineweaver–Burk plot involve convex-upward and convex-downward hyperbola portions, respectively, suggestive of positive cooperativity of L binding), which leads to incorrect N and K. Errors in N and K would depend on (i) the binding (K, N and kn) and method (α) parameters and (ii) the expressions used to calculate approximate B_S and U values. Simulations involving variable α, KN and kn values indicate that: (1) the magnitude of error in N determination (mainly involving moderate underestimation) directly depends on the α value; (2) the magnitude of K underestimation mainly depends on the KN value; it is moderate (usually < two-fold) with KN values < 1, but could become very high (e.g. >100-fold), when $KN > 10^2$. In this case, the K underestimation is modulated by the α and kn values. Practical situations which afford high KN and thus might result in very marked underestimation of K are discussed. A single R dilution method is proposed to assess the validity of K determinations using the R saturation analysis approach.

Keywords: Binding site; Saturation analysis; Equilibrium association constant

1. Introduction

The determination of binding parameters (affinity binding constant, receptor concentration, etc.) relative to receptor/ligand interactions constitutes a basic operation in many areas of endocrinology. Determination of these parameters could be very useful, e.g. to analyze physiopathological situations or evaluate new ligands synthesized to obtain more potent or selective receptor agonists or antagonists. In cell-free systems, a considerable number of studies have therefore been devoted to the determination of such binding parameters. One of the most common approaches involves saturation experiments where the specific binding of increasing concentrations of a radioactive ligand to a receptor-containing cell extract is determined under equilibrium or pseudo-equilibrium conditions. This approach – via graphical representation or computational analysis of binding data – should allow determination of the specific binding site concentration, the equilibrium affinity constant, and could reveal

* Tel.: +33 4 67 04 37 14; fax: +33 4 67 54 05 98.
E-mail address: borgna@montp.inserm.fr.

0960-0760/$ – see front matter © 2004 Elsevier Ltd. All rights reserved.
doi:10.1016/j.jsbmb.2004.08.004

Nomenclature

R	receptor
L	(radioactive) ligand
K	equilibrium association constant
N	specific binding site (or R) concentration in the cell extract
kn	equilibrium nonspecific binding coefficient
T	total concentration of L
B_S	concentration of specifically bound L (or RL complex concentration) at equilibrium
B_{NS} and B'_{NS}	concentrations of nonspecifically bound L at equilibrium (in the absence and presence of an excess of unlabeled L, respectively)
U and U'	concentrations of unbound L at equilibrium (in the absence and presence of an excess of unlabeled L, respectively)
B_1 and B_2	measured L concentrations after running a procedure to separate bound and unbound L from equilibrated media not-containing and containing unlabeled L, respectively
α, β and γ	proportions of B_S, B'_{NS} (or B'_{NS}), and U (or U') measured after running the separation procedure
B_S^a and B_S^b	calculated underestimates of B_S (cf. appendix for definition)
U^a, U^b, U^c and U^d	calculated overestimates of U (cf. appendix for definition)
ϕ and ψ	are $(1-\beta)kn+1-\gamma$ and $(\alpha-\beta)kn+\alpha-\gamma$, respectively
X_o and Y_o	intercepts on axes of the Scatchard graph related to the R/L interaction
S_o	Y_o/X_o ratio
X_r and Y_r	intercepts on axes of a least-squares straight regression line established from a set of Scatchard graph points
S_r	Y_r/X_r ratio

multiple sets of binding sites or cooperative or noncooperative receptor/ligand binding. However, graphical representations or computational analysis can be validly interpreted only if the data derived from saturation experiments are not distorted by methodological errors. On the basis of papers on the theory of protein/ligand interactions that were published in the 1970 and 80s, the effects (mainly qualitative) of the most common artefacts on graphical representation of the R/L interaction were analyzed. Such common artefacts involve ligand radiochemical impurity [1–4], ligand or receptor degradation or capture [4–8], incomplete recovery of the receptor:ligand complex [4,7,8] and non-equilibrium binding conditions [4,8]. These artefacts could result in underestimation of the equilibrium association constant, and sometimes in misinterpretation, concerning the number of involved receptor species or the cooperative or noncooperative type of receptor/ligand interactions.

The considerable discrepancies between values reported for binding parameters of the estrogen receptor α/estradiol interaction clearly illustrate the difficulties that could be encountered for reliable determination of such parameters. Saturation analyses using [^{3}H]estradiol have usually led to 10^9–10^{10} M^{-1} K_a values, whereas the ratio of the kinetic association rate constant to the dissociation rate constant was almost two orders higher [9,10]. Moreover, with the receptor concentrations used (nM range), Scatchard transforms of estradiol binding data were frequently convex curvilinear suggesting positive cooperativity of estradiol binding [11,12], whereas with much lower receptor concentrations (0.01 nM range) Scatchard plots of 16α-iodoestradiol binding were linear, indicating a single class of binding sites, leading to a K_a value $\geq 10^{11}$ M^{-1} [12].

For a large variety of R/L systems, most R saturation analyses devoted to the determination of K and N involve a procedure (filtration, adsorption, precipitation...) for the separation of bound and unbound L. The procedure used could change the equilibrium concentrations of specifically bound, nonspecifically bound and unbound L. Moreover, an approximate expression ("$B_1 - B_2$", cf Working hypotheses in the next section) is generally used to calculate the specifically bound L concentration from binding measurements. These two facts could lead to erroneous K and N.

In the late 1970s, on the basis of results obtained in estrogen receptor/ligand binding studies, we proposed [13] reliable calculations of specifically bound and unbound L concentrations which, in addition to the L binding measurements, involved two parameters, i.e. kn, the nonspecific binding coefficient, and α, the proportion of equilibrium RL concentration measured under pseudo-equilibrium conditions (cf. Working hypotheses). For the simplest R/L interaction model, this paper mainly examines the effects of incorrect L specific binding calculations resulting from α and/or kn neglect, on the determination of binding parameters via saturation analysis. This investigation indicates that when KN is high there could be considerable underestimation of the binding constant as a result of inaccurate determination of specific binding.

2. Results

2.1. Working hypotheses

The theory of protein/ligand interactions, involving ligand specific and nonspecific binding, has been discussed by many authors (e.g. Rodbard [14] and Rodbard and Feldman [15]). However, to provide a background for the present investigation, the basis of the saturation analysis approach and the main graphical characteristics of specific and nonspecific binding will be briefly reviewed.

The simplest binding process of a ligand (L) to its cognate receptor (R) in a cell-free system is:

$$\mathrm{R} + \mathrm{L} \underset{k_2}{\overset{k_1}{\rightleftarrows}} \mathrm{RL}$$

where L molecules stoechiometrically associate with equivalent and independent binding sites on R molecules, according to a bimolecular process (rate constant, k_1) and dissociate from these sites according to a monomolecular process (rate constant, k_2). The characteristics of such a binding process, defined as L specific binding, is high affinity (reflecting R/L specific recognition) and saturability (resulting from the presence of a discrete number of L binding sites on R). In practice, R-containing cell extracts include a wide variety of molecular species, many of which nonspecifically interact with L and, although the nature of this nonspecific binding is not clearly understood, it is characterized by low affinity and very high capacity, with linear nonsaturable binding up to L concentration $\geq 10^{-5}$ M [13–16].

Then, we will consider that the incubation of a R-containing cell extract with a given concentration of L under equilibrium conditions results in L specific and nonspecific binding whose respective concentration B_S and B_NS are such that:

$$B_\mathrm{S} = \frac{KNU}{KU+1} \tag{1}$$

and

$$B_\mathrm{NS} = knU \tag{2}$$

where $K = k_1/k_2$ is the equilibrium association constant for the R/L interaction, N is the specific binding site concentration (and the R concentration when each R molecule harbors only one L binding site), kn is the equilibrium nonspecific binding coefficient, and U is the concentration of unbound L. When increasing concentrations of L are used, the resulting binding data should allow determination of the various binding parameters. Such binding data related to specific binding, nonspecific binding, and both, represented by Michaelis–Menten and Scatchard plots, are shown in Fig. 1.

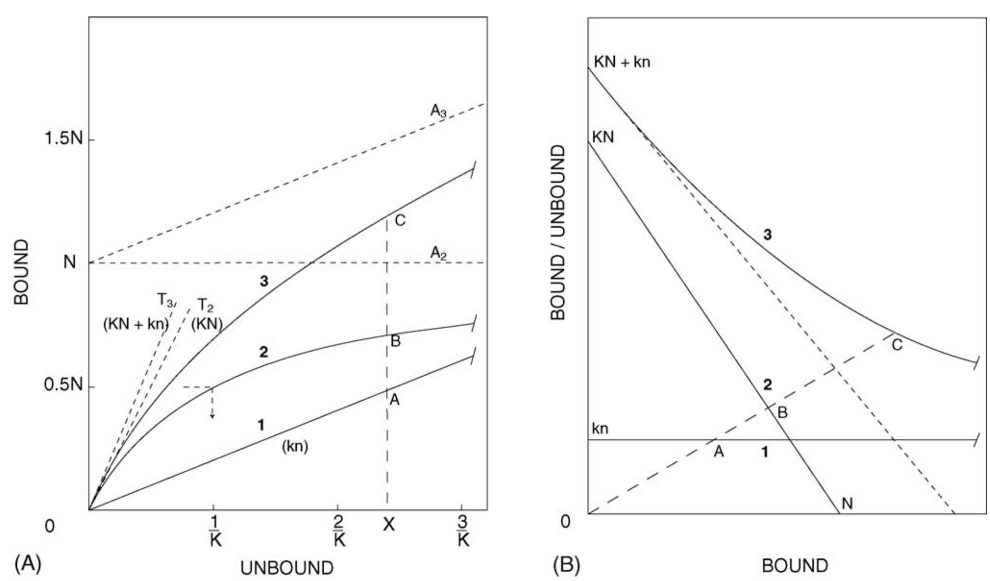

Fig. 1. Michaelis–Menten and Scatchard graphs of specific and nonspecific binding under equilibrium conditions. (A) The Michaelis–Menten plot of the nonsaturable binding (assimilated to nonspecific binding) of a ligand L in cell extracts under equilibrium conditions gives rise to straight line **1**, related to equation $B_\mathrm{NS} = knU$, where kn characterizes the L nonspecific binding in extracts. The plot of L binding to a receptor R (simplest R/L interaction) under equilibrium leads to an equilateral hyperbola portion **2**, related to equation $B_\mathrm{S} = KNU/(KU+1)$. The ordinate of the hyperbola asymptote (A_2) is N and the slope of the tangent to hyperbola at the origin (T_2) is KN. The Michaelis–Menten plot of L total binding ($B_\mathrm{S} + B_\mathrm{NS}$) leads to a hyperbola portion **3** related to equation $B_\mathrm{S} + B_\mathrm{NS} = (KNU/(KU+1)) + knU$. The intercept on the ordinate axis of the hyperbola asymptote (A_3) is N and the slope of the tangent to hyperbola at the origin (T_3) is $KN + kn$. Note that intercepts X, A, B and C of any parallel to the ordinate axis on the abscissa axis, and **1**, **2** and **3**, respectively, verify $XC = XA + XB$. (B) The Scatchard plot of L nonspecific binding gives rise to straight line **1**, related to $B_\mathrm{NS}/U = kn$. The plot of L binding to R leads to a straight line segment **2**, related to equation $B_\mathrm{S}/U = K(N - B_\mathrm{S})$. The segment intercepts on abscissa and ordinate axes are N and KN, respectively, and the slope is K. The Scatchard plot of L total binding ($B_\mathrm{S} + B_\mathrm{NS}$) leads to a hyperbola segment **3**, related to equation $(B_\mathrm{S} + B_\mathrm{NS})/U = (1/2)(K[N - (B_\mathrm{S} + B_\mathrm{NS})] + kn + \sqrt{(K[N - (B_\mathrm{S} + B_\mathrm{NS})] + kn)^2 + 4Kkn(B_\mathrm{S} + B_\mathrm{NS})})$ (cf. Appendix). The hyperbola intercept on the ordinate axis is ($KN + kn$) and lines **1** and **2** constitute hyperbola asymptotes. Note that (i) intercepts A, B and C of any straight line stems from the axis origin (O) on **1**, **2** and **3**, respectively, are such that OC = OA + OB, and (ii) the slope of the tangent to hyperbola at the intercept on the ordinate axis (short dashed line) is lower than K, whereas the tangent intercept on the abscissa axis is higher than N; therefore linear extrapolations made from the left part of the curve lead to erroneous K and N. (A) and (B) Provided that $KN = 5kn$ (5 is the value selected for the KN/kn ratio to illustrate L specific and nonspecific binding), curves **1**, **2** and **3** could account for B_S, B_NS and $B_\mathrm{S} + B_\mathrm{NS}$ related to various values of K, N and kn. Unchanged representation **2** of L binding to R could be obtained when equilibrium B_S and U are calculated from binding data B_1 and B_2 obtained after running a separation method of bound and unbound L (even if a portion of the RL complex is lost when this method is performed), using Eqs. (9) and (10). This requires prior determination of the nonspecific binding parameter kn and the method parameter α.

The Michaelis–Menten plot of the R/L interaction (B_S as a function of U) is constituted by a portion of equilateral hyperbola (curve **2** in Fig. 1A) corresponding to Eq. (1). The limit value for B_S (materialized by the horizontal asymptote to the curve) is N, whereas the slope of the tangent to the hyperbola at the origin is KN. Then K could be determined as the ratio of the two above parameters. The Scatchard plot of the R/L interaction (B_S/U as a function of B_S) is constituted by a straight line segment (line **1** in Fig. 1B) corresponding to equation:

$$\frac{B_S}{U} = K(N - B_S). \tag{3}$$

The intercepts of the straight line on abscissa and ordinate axes are N and KN, respectively; its slope is K.

In the present investigation, we assume that (i) both R and L are homogeneous, and (ii) equilibrium binding (specific and nonspecific) is reached before a procedure is run to separate bound and unbound L in order to gain access to B_S and U. To determine B_S and B_{NS} for a given concentration of radiolabeled L (T), two parallel incubations of the R preparation with L are usually performed, one in the absence, and the other in the presence of a large excess of unlabeled L (concentration T°, such as $T^\circ \geq 100\,N$ and $T^\circ \geq 100\,T$, to nullify the binding of radiolabeled L to R). In cases where the two parallel incubations are carried out in dialysis cells, the bound and unbound radioligand concentrations at equilibrium could be measured directly. However, performing equilibrium dialysis is laborious and could afford a high level of nonspecific binding. Therefore, alternative and more versatile methods involving filtration, adsorption, chromatography, precipitation, etc., are used, which ideally induce the separation of bound ($B_S + B_{NS}$ and B'_{NS}, in the first and second incubations, respectively) and unbound L (U, and U', respectively) while strongly decreasing L nonspecific binding. Let us call B_1 and B_2 the concentrations of L recovered after running the separation method from equilibrated samples not-containing and containing unlabeled L, respectively. Since the separation procedure is applied to aliquots involving B_S, B_{NS} and U (or B'_{NS} and U'), and since most of the separation procedures are not completely selective and not fully quantitative [12,13,17–20], in the B_1 and B_2 expressions, correction coefficients α, β and γ (each ≤ 1), which depend on the type of separation procedure used and on the particular R and L pair studied, are assigned to the equilibrium concentrations of bound and unbound L:

$$B_1 = \alpha B_S + \beta B_{NS} + \gamma U \tag{4}$$

and

$$B_2 = \beta B'_{NS} + \gamma U' \tag{5}$$

whereas

$$T = B_S + B_{NS} + U \tag{6}$$

and

$$T = B'_{NS} + U' \tag{7}$$

with $B_{NS} = knU$ (Eq. (2)) and

$$B'_{NS} = knU', \tag{8}$$

As previously demonstrated [13], from Eqs. (2) and (4)–(8), B_S and U can be expressed as:

$$B_S = (B_1 - B_2)\frac{T}{\alpha T - B_2} \tag{9}$$

and

$$U = \frac{\alpha T - B_1}{\alpha T - B_2} \times \frac{T}{kn + 1}. \tag{10}$$

The calculation of B_S and U from T, B_1 and B_2 does not involve β, and γ parameters but requires preliminary determination of α and (only for the calculation of U) kn. Determination of α could be done by performing two parallel equilibrium dialyses with the R preparation and a given concentration of radiolabeled L, in the absence and presence of unlabeled L, respectively, and then submitting aliquots from the protein-containing dialysis compartments to the separation process. Comparison of binding data obtained on one hand by dialysis and on the other hand by the separation process will allow calculation of α [13]. Determination of kn could be made by performing a single equilibrium dialysis of the R preparation with radioactive L in the presence of a large excess of unlabeled L [13].

2.2. Consequences of common approximations in the determination of equilibrium bound and unbound ligand concentrations on the calculation of N and K

As stated above, accurate determination of B_S and U from B_1, B_2 and T requires prior determination of the separation method parameter α and the cell extract nonspecific binding parameter kn. Inaccurate determination of B_S and U could lead to graphical representations of binding data which do not reflect the actual R/L interaction, with possible incorrect N and K determinations and erroneous interpretation of the noncooperative type of binding. We will examine the effect resulting from α and/or kn neglect on N and K determination by means of saturation experiments, using mainly Michaelis–Menten and Scatchard representations of the binding data.

2.2.1. Effect of kn neglect

When α but not kn has been determined, then B_S can be calculated from T, B_1, B_2 and α using Eq. (9), whereas U^a, an overestimate by factor $(kn+1)$ of U, could be calculated from the same terms by neglecting kn in Eq. (10):

$$U^a = \frac{\alpha T - B_1}{\alpha T - B_2}T = T - B_S = (kn+1)U. \tag{11}$$

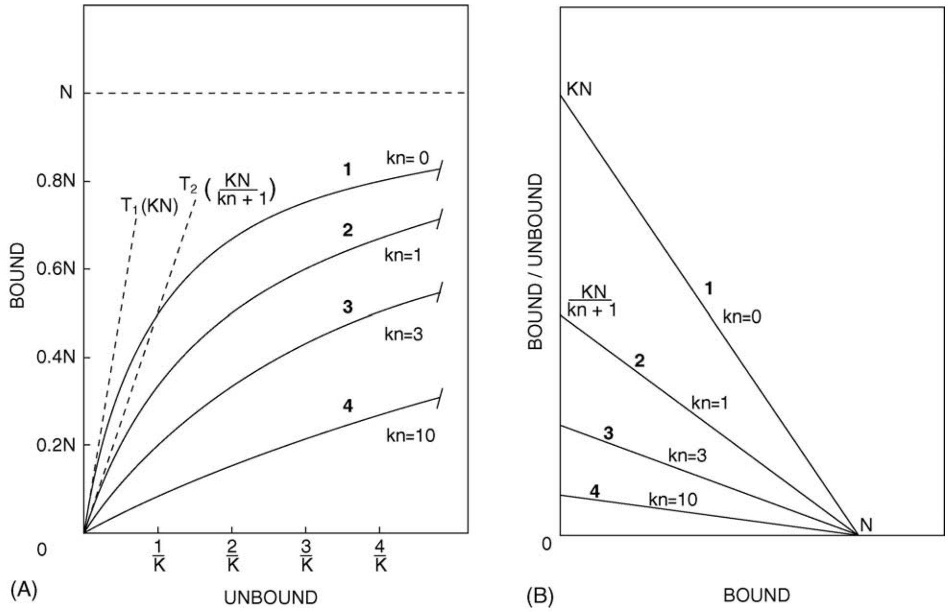

Fig. 2. Michaelis–Menten and Scatchard graphs of specific binding when the nonspecific binding parameter kn is not taken into account. Accurate calculation of equilibrium B_S (Eq. (9)) and U (Eq. (10)) from T and the binding measurements, B_1 and B_2 made after running a separation process of bound and unbound L, requires prior determination of α and kn. The various Michaelis–Menten (A) or Scatchard (B) plots of a simple R/L interaction obtained when α has been determined and kn (selected values: 1, 3 and 10) has been or not determined, are shown. (A) When kn has been determined (or $kn = 0$) a regular plot is obtained which involves a portion of equilateral hyperbola **1** whose upper limit materialized by asymptote is N and slope of the tangent to hyperbola at the origin (T_1) is KN. When kn (>0) has not been determined, Eq. (11), which affords U^a an overestimate of U by factor ($kn+1$), could be used instead of Eq. (10). The corresponding Michaelis–Menten plot (B_S as a function of U^a) consists of another equilateral hyperbola portion (illustrated by curves **2**, **3** and **4**, corresponding to $kn = 1$, 3 and 10, respectively) whose upper limit is still N, whereas the slope of the tangent to hyperbola at the origin is $KN/(kn+1)$, suggesting an apparent K value of $K/(kn+1)$. (B) The regular Scatchard plot obtained when kn has been determined (or $kn = 0$) involves a straight line segment **1** defining N and KN on abscissa and ordinate axes, respectively. When kn (>0) has not been determined, the corresponding Scatchard plot (B_S/U^a as a function of B_S) consists of another straight line segment (illustrated by segments **2**–**4**) whose intercept on the abscissa axis is still N, whereas that on the ordinate axis is $KN/(kn+1)$, suggesting an apparent K value of $K/(kn+1)$. (A) and (B) Relative to that of the regular curve **1** positions of curves **2**–**4** are independent of the N and K values.

Then Eqs. (1) and (3) give:

$$B_S = \frac{KNU^a}{KU^a + kn + 1} \tag{12}$$

$$\frac{B_S}{U^a} = \frac{K}{kn+1}(N - B_S). \tag{13}$$

B_S is represented as a function of U^a by a portion of equilateral hyperbola whose slope of the tangent at the origin is $KN/(kn+1)$ and whose limit value is N (Fig. 2A). Similarly, B_S/U^a is represented as a function of B_S by a straight line segment whose intercepts on the abscissa and ordinate axes are N and $KN/(kn+1)$, respectively (Fig. 2B). Irrespective of the representation used, the neglect of kn, therefore has no incidence on the calculated binding site concentration or on the apparent type (noncooperative) of R/L interaction, but it results in underestimation of the equilibrium association constant by factor ($kn+1$). Obviously identical results would be obtained by using other types of representations, e.g. the Lineweaver–Burk plot ($1/B_S$ as a function of $1/U^a$) and the $B_S = f(T)$ plot (not shown). Note that in the examined context, except when $\alpha = 1$, the use of another approximate expression of U:

$$U^b = T - B_1 \tag{14}$$

would generate less favourable binding data for graphical representation of the R/L interaction than those obtained by using U^a (cf. Appendix).

2.2.2. Effect of α neglect

When kn but not α ($\alpha < 1$) has been determined, neither B_S nor U could be calculated. Neglecting α in Eqs. (9) and (10) affords approximate expressions of B_S and U, i.e.:

$$B_S^a = (B_1 - B_2)\frac{T}{T - B_2} \tag{15}$$

and

$$U^c = \frac{T - B_1}{T - B_2} \times \frac{T}{kn+1} = \frac{T - B_S^a}{kn+1}. \tag{16}$$

B_S^a is an underestimation of B_S by factor $(T - B_2)/(\alpha T - B_2)$ (>1), whereas U^c is an overestimation of U by factor $((T - B_1)/(\alpha T - B_1)) \times ((\alpha T - B_2)/(T - B_2))$ (>1). Note that there are two other possible approximate expressions of U, U^b (already defined in the preceding section) and

$$U^d = T - B_S^a. \tag{17}$$

However, provided that $kn > (\gamma/(1-\beta))$ (a condition that almost always applies) $U^d > U^b > U^c$ (cf. Appendix). Then the use of U^b or U^d instead of U^c would lead to less favourable representations, $B_S = f(U)$ or $B_S/U = f(B_S)$, of the R/L interaction.

Expression of B_S^a as a function of U^c and expression of B_S^a/U^c as a function of B_S^a (cf. Appendix) involve all three binding parameters and all three method parameters:

$$B_S^a = \frac{\psi[(1-\alpha)KN + \phi(1+KU^c)]}{2(1-\alpha)K\phi} - \frac{\psi\sqrt{[(1-\alpha)KN + \phi(1+KU^c)]^2 - 4\phi(1-\alpha)K^2NU^c}}{2(1-\alpha)K\phi} \quad (18)$$

and

$$\frac{B_S^a}{U^c} = \frac{\psi K(\psi N - \phi B_S^a)}{(1-\alpha)K(\psi N - \phi B_S^a) + \phi\psi} \quad (19)$$

where

$$\phi = (1-\beta)kn + 1 - \gamma \quad (20)$$

and

$$\psi = (\alpha-\beta)kn + \alpha - \gamma. \quad (21)$$

When $\alpha < 1$, irrespective of the β, γ and kn values (even 0), B_S^a and B_S^a/U^c are hyperbolic functions of U^c and B_S^a, respectively. Then the corresponding Michaelis–Menten and Scatchard plots (Fig. 3) involve convex-upward portions of hyperbolae (the hyperbola is equilateral only in the case of the Scatchard representation). Using the Michaelis–Menten plot, when $U^c \to \infty$ the B_S^a limit (apparent N) is $N(\psi/\phi)$, whereas the slope of the tangent to hyperbola at the origin (apparent KN) is $KN(\psi/((1-\alpha)KN+\phi))$ (Fig. 3A). So the apparent K calculated from these two parameters is $K(\phi/((1-\alpha)KN+\phi))$. Using the Scatchard plot, the obtained curve suggests positive cooperativity for L binding to R (i.e. Hill coefficient $n > 1$). Intercepts of the hyperbola with coordinate axes are $X_o = N(\psi/\phi)$ and $Y_o = KN(\psi/((1-\alpha)KN+\phi))$, respectively (Fig. 3B), so the slope of the straight line defined by the two intercepts is $S_o = K(\phi/((1-\alpha)KN+\phi))$.

Then X_o, Y_o and S_o are identical to the apparent N, the apparent KN and the apparent K, deduced from the direct representation of B_S^a as a function of U^c. Since $\phi > \psi$ (pro-

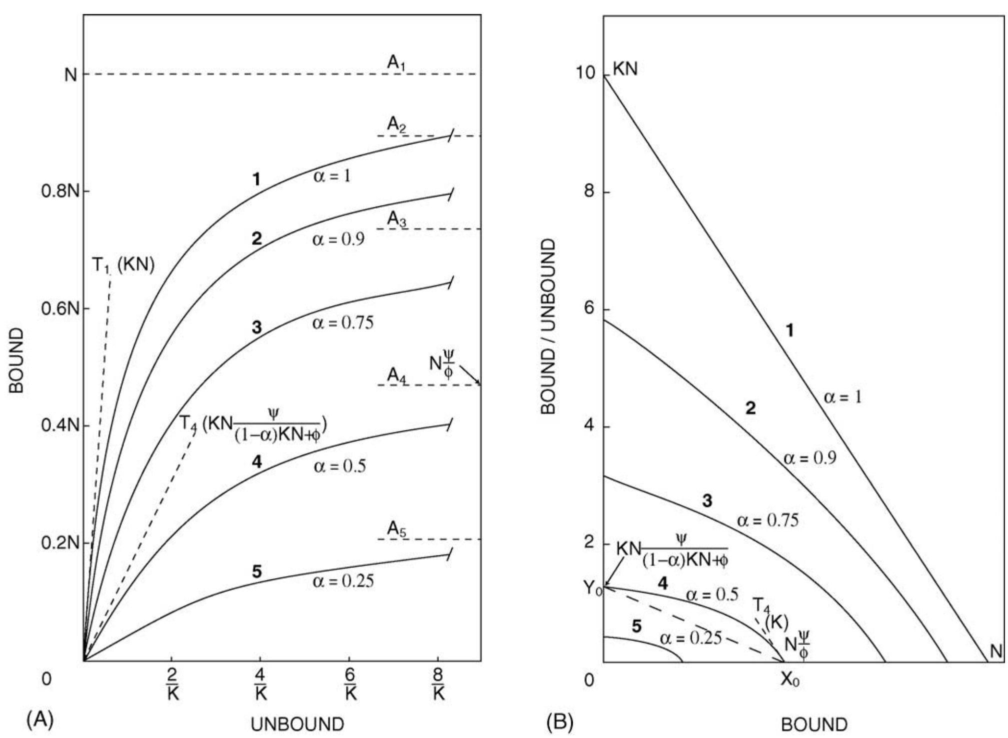

Fig. 3. Michaelis–Menten and Scatchard graphs of specific binding when the method parameter α is not taken into account. When the binding parameter kn but not the method parameter α ($\alpha \neq 1$) has been determined, Eqs. (15) and (16) which give B_S^a and U^c, an underestimate of B_S and an overestimate of U, respectively, could be used. Then for a simple R/L interaction, representation of binding data according to Michaelis–Menten (B_S^a as a function of U^c, (A)) or Scatchard (B_S^a/U^c as a function of B_S^a, (B)) involves a convex-upward portion of hyperbola whose characteristics are determined by the binding (K, N and kn) and method (α, β and γ) parameter values. Four hyperbola segments **2**–**5** obtained for selected values of KN (10), kn (1), β (0.1), γ (0.01) and various values of α (0.9, 0.75, 0.5 and 0.25) are shown together with the regular hyperbola portion **1** (A) or the straight line segment **1** (B) obtained when $\alpha = 1$ (or when $\alpha \neq 1$ has been determined, and Eqs. (9) and (10) are used to exactly calculate B_S and U). (A) The hyperbola upper limit, materialized by a portion of asymptote (A_1 to A_5, for $\alpha = 1$ to $\alpha = 0.25$) is $N(\psi/\phi)$, where $\psi = (\alpha-\beta)kn + \alpha - \gamma$ and $\phi = (1-\beta)kn + 1 - \gamma$; the slope of the tangent to hyperbola at the origin (only specified for curves **1** and **4**: T_1 and T_4) is $KN(\psi/((1-\alpha)KN+\phi))$ (or KN, when $\alpha = 1$). (B) The hyperbola intercept on the abscissa axis is $X_o = N(\psi/\phi)$, whereas the intercept on the ordinate axis is $Y_o = KN(\psi/((1-\alpha)KN+\phi))$. The slope of the straight line defined by hyperbola intercepts on axes and that of the tangent to hyperbola at the intercept on the abscissa axis are $S_o = K(\phi/((1-\alpha)KN+\phi))$ and K, respectively. (A) and (B) With the selected values for α, β, γ and kn parameters, hyperbolae fit with any value of N, provided that the corresponding K is equal to $10/N$.

Table 1
Apparent K/K ratios resulting from α neglect-effects of α and KN

S_o/K		α				
$\mathbf{S_r/K}$		0.25	0.5	0.75	0.9	1
KN	10^{-2}	0.996	0.997	0.999	0.999	1
		0.996 (r > **0.99**)	**0.997** (r > **0.99**)	**0.999** (r > **0.99**)	**0.999** (r > **0.99**)	**1**
	10^{-1}	0.962	0.974	0.987	0.995	1
		0.962 (r > **0.99**)	**0.974** (r > **0.99**)	**0.987** (r > **0.99**)	**0.995** (r > **0.99**)	**1**
	1	0.715	0.791	0.883	0.950	1
		0.713 (r > **0.99**)	**0.789** (r > **0.99**)	**0.883** (r > **0.99**)	**0.950** (r > **0.99**)	**1**
	10	0.201	0.274	0.431	0.654	1
		0.182 (r = **0.90**)	**0.256** (r = **0.93**)	**0.418** (r = **0.97**)	**0.649** (r = **0.99**)	**1**
	10^2	0.0246	0.0364	0.0703	0.159	1
		0.0181 (r = **0.74**)	**0.0275** (r = **0.75**)	**0.0562** (r = **0.80**)	**0.140** (r = **0.88**)	**1**
	10^3	0.00251	0.00377	0.00750	0.0185	1
		0.00175 (r = **0.70**)	**0.00263** (r = **0.70**)	**0.00530** (r = **0.71**)	**0.0135** (r = **0.73**)	**1**

When α ($\alpha \neq 1$) has not been determined, Eqs. (15) and (16), which give B_S^a and U^c an underestimate of B_S and an overestimate of U, respectively, could be used. Then for a simple R/L interaction, there are hyperbolic relations between the corresponding Michaelis–Menten coordinates (B_S^a and U^c) or Scatchard coordinates (B_S^a/U^c and B_S^a). From hyperbola related to Michaelis–Menten or Scatchard coordinates two parameters S_o and S_r (cf. Figs. 3 and 4) are considered. S_o ($S_o = K(\phi/((1-\alpha)KN+\phi))$, where $\phi = (1-\beta)kn+1-\gamma$) is the slope of the straight line defined by intercepts on the abscissa and the ordinate axes of hyperbola obtained in the Scatchard plot; it is also the apparent K deduced from the direct representation of B_S^a as a function of U^c (cf. Appendix). In the Scatchard plot S_r is the slope of the least-squares straight regression line defined by 10 hyperbola points (selected as indicated in the Fig. 4 legend); S_r is the apparent K deduced from these 10 Scatchard coordinates. For constant values of β (0.1), γ (0.01) and kn (1) parameters and various α and KN pairs of values, S_o and S_r were calculated as functions of K. The values of S_o/K (normal numbers) and S_r/K (bold numbers) ratios are given for the various α and KN pairs of values. The correlation coefficient of each S_r-related regression line is mentioned in brackets. Note that the use of Eqs. (15) and (14) (B_S^a and U^b) or Eqs. (23) and (14) (B_S^b and U^b) instead of (15) and (16) to calculate approximate values of B_S and U, would change the values of S_o/K and S_r/K ratios by factor $1/\phi$ (i.e. 0.529 with values attributed to β, γ and kn).

vided that $\alpha < 1$), apparent N, apparent KN and apparent K are always lower than N, KN and K, which would be obtained by taking α into account in the B_S and U calculations. It is noteworthy that the (apparent N)/N ratio involves neither N nor K but is an increasing function of α and a decreasing function of kn (provided that $\gamma < \beta$), whereas the (apparent K)/K ratio is a decreasing function of KN and an increasing function of α and ϕ or kn (variations in X_o/N and S_o/K, according to α, KN and kn will be presented further in Tables 1–4). This suggests that both α and KN play major roles in defining the characteristics of hyperbolae. For various values of α and given values of the other parameters (involving $KN = 10$), Fig. 3A and B show the hyperbola portions obtained using Michaelis–Menten plot and Scatchard plot, respectively. As α decreases, the hyperbola portion becomes increasingly distant from the regular curve accounting for the R/L interaction. Note that in practice the random distribution of experimental errors will overlap the systematic deviations resulting from α neglect and could more or less mask such deviations.

Since simple algebraic manipulations convert one plot to another plot, the same intrinsic apparent N and apparent K could be obtained by using other plots, e.g. the Lineweaver–Burk plot (cf. Appendix) and the $B_S^a = f(T)$ plot (not shown); the latter instead of overestimated U (used in the above representations) involving T, which in the present investigation was not hampered by any misestimation. However, α neglect has different effects on Michaelis–Menten and $B_S = f(T)$ plots (regular hyperbola is changed to another hyperbola) and Scatchard and Lineweaver–Burk plots (regular straight line is changed to hyperbola). These latter situations

Table 2
Apparent N/N ratios resulting from α neglect-effects of α and KN

X_o/N		α				
$\mathbf{X_r/N}$		0.25	0.5	0.75	0.9	1
KN	10^{-2}–10^3	0.206	0.471	0.735	0.894	1
	10^{-2}	**0.206**	**0.471**	**0.736**	**0.894**	**1**
	10^{-1}	**0.208**	**0.473**	**0.737**	**0.895**	**1**
	1	**0.218**	**0.489**	**0.750**	**0.902**	**1**
	10	**0.268**	**0.582**	**0.844**	**0.958**	**1**
	10^2	**0.334**	**0.743**	**1.10**	**1.20**	**1**
	10^3	**0.351**	**0.798**	**1.24**	**1.46**	**1**

For a simple R/L interaction, the use of Eqs. (15) (B_S^a) and (16) (U^c) instead of Eqs. (9) and (10) to calculate B_S and U, results in hyperbolic relations between Scatchard or Michaelis–Menten coordinates. From hyperbola related to Michaelis–Menten or Scatchard coordinates, two parameters X_o and X_r (cf. Figs. 3 and 4) are considered. X_o ($X_o = N(\psi/\phi)$, where $\psi = (\alpha-\beta)kn+\alpha-\gamma$ and $\phi = (1-\beta)kn+1-\gamma$) is the intercept on the abscissa axis of the hyperbola obtained in the Scatchard plot; X_o is also the apparent N deduced from the direct representation of B_S^a as a function of U^c (cf. Appendix). In the Scatchard plot X_r is the intercept of the least-squares regression line, defined by ten hyperbola points described in the Table 1 and Fig. 4 legends; X_r is the apparent N deduced from these ten Scatchard coordinates. For constant values of β (0.1), γ (0.01) and kn (1) parameters and various α and KN pairs of values, X_o and X_r were calculated as functions of N. The values of X_o/N (normal numbers) and X_r/N (bold numbers) ratios are given for the various α and KN pairs of values. Note that the use of Eqs. (15) and (14) (U^b) instead of Eqs. (15) and (16) to calculate approximate values of B_S and U, would not change the X_o/N and X_r/N values given in the Table, whereas the use of Eqs. (23) (B_S^b) and (14) would change the values of the two ratios by factor $\phi/(kn+1)$ (i.e. 0.945 with values attributed to β, γ and kn).

Table 3
Apparent K/K ratios resulting from α neglect-modulation of the effects of α and KN by kn

S_o/K		kn		
$\mathbf{S_r/K}$		0.1	1	10
$KN = 1$	$\alpha = 0.5$	0.684	0.791	0.952
		0.676 ($r > $ **0.99**)	**0.788** ($r > $ **0.99**)	**0.952** ($r > $ **0.99**)
	$\alpha = 0.75$	0.812	0.883	0.976
		0.810 ($r > $ **0.99**)	**0.882** ($r > $ **0.99**)	**0.976** ($r > $ **0.99**)
	$\alpha = 0.9$	0.915	0.950	0.990
		0.915 ($r > $ **0.99**)	**0.950** ($r > $ **0.99**)	**0.990** ($r > $ **0.99**)
$KN = 100$	$\alpha = 0.5$	0.0211	0.0364	0.167
		0.0114 ($r = $ **0.61**)	**0.0215** ($r = $ **0.67**)	**0.135** ($r = $ **0.88**)
	$\alpha = 0.75$	0.0414	0.0703	0.286
		0.0250 ($r = $ **0.68**)	**0.0473** ($r = $ **0.76**)	**0.256** ($r = $ **0.94**)
	$\alpha = 0.9$	0.0975	0.159	0.500
		0.0705 ($r = $ **0.81**)	**0.128** ($r = $ **0.87**)	**0.483** ($r = $ **0.98**)

For a simple R/L interaction, the use of Eqs. (15) (B_S^a) and (16) (U^c) to calculate B_S and U, results in hyperbolic relations between Michaelis–Menten or Scatchard coordinates. The S_o and S_r parameters (described in the Table 1 legend) were calculated as functions of K for constant values of β (0.1) and γ (0.01) and various values of α, KN and kn. Each S_r value was derived from a least-squares regression line defined by eleven hyperbola points having the following abscissae 0, $0.1N(\psi/\phi)$, $0.2N(\psi/\phi)$ ..., $N(\psi/\phi)$, where $\psi = (\alpha - \beta)kn + \alpha - \gamma$ and $\phi = (1 - \beta)kn + 1 - \gamma$. The values of S_o/K (normal numbers) and S_r/K (bold numbers) ratios, which represent the (apparent K)/K ratio in Michaelis–Menten plots and Scatchard plots, respectively, are given for the various values of kn, KN and $k\alpha$. The correlation coefficient of each S_r-related straight line is mentioned in brackets. The note in the last part of the Table 1 legend, related to the use of Eqs. (15) and (14) (U^b) or Eqs. (23) (B_S^b) and (14) instead of Eqs. (15) and (16), still applies for the S_o/K and S_r/K ratio values in the Table.

would have practical consequences on the determination of apparent N and apparent K. For instance, using the Scatchard plot, when a linear relationship between B_S/U and B_S is expected, reflecting a postulated R/L simple interaction, the usual way to determine N and K is to establish the least-squares straight regression line corresponding to a set of B_S and B_S/U pairs derived from step-wise R saturation experiments. A regression line defined from a set of B_S^a and B_S^a/U^c pairs from the Scatchard hyperbola segment would afford an apparent $N(X_r)$ and an apparent $KN(Y_r)$ on abscissa and ordinate axes, respectively, and then an apparent K equal to the slope $S_r = Y_r/X_r$ of the regression line (Figs. 4 and 5). Depending on the B_S^a and B_S^a/U^c pairs used, X_r and S_r could vary and then more or less differ from X_0 and S_0 (with $X_r \geq X_0$ and usually $S_r \leq S_0$). However, when an appropriate set of adequately incremented B_S^a and B_S^a/U^c pairs (which fairly well account for the whole hyperbola segment) are used, the corresponding X_r (Tables 2 and 4) and S_r (Tables 1 and 3) are close to X_0 and S_0, respectively. Then, regardless of the plot used, apparent N (i.e. intrinsic X_0 or X_r) and apparent K (i.e. intrinsic S_0 or S_r) should not markedly vary. Therefore, to condense this study, only the Scatchard representation (with related X_0, X_r, S_0 and S_r parameters), which involves the simplest relation between the graphical coordinates will be considered hereafter (Figs. 4–6).

Table 4
Apparent N/N ratios resulting from α neglect-modulation of the effects of α and KN by kn

X_o/N		kn		
$\mathbf{X_r/N}$		0.1	1	10
$KN = 1$	$\alpha = 0.5$	0.491	0.471	0.449
		0.521	**0.488**	**0.453**
	$\alpha = 0.75$	0.745	0.735	0.725
		0.770	**0.750**	**0.727**
	$\alpha = 0.9$	0.898	0.894	0.890
		0.910	**0.901**	**0.891**
$KN = 100$	$\alpha = 0.5$	0.491	0.471	0.449
		1.04	**0.919**	**0.635**
	$\alpha = 0.75$	0.745	0.735	0.725
		1.42	**1.26**	**0.910**
	$\alpha = 0.9$	0.898	0.894	0.890
		1.43	**1.28**	**1.00**

For a simple R/L interaction, the use of Eqs. (15) (B_S^a) and (16) (U^c) to calculate B_S and U results in hyperbolic relations between Michaelis–Menten or Scatchard coordinates. The parameters X_o and X_r (the latter derived from the least-squares regression line mentioned in the Table 3 legend) described in the Table 2 legend, were calculated as a function of N for constant values of β (0.1) and γ (0.01) and various values of α, KN and kn. The values of X_o/N (normal numbers) and X_r/N (bold numbers) ratios, which represent the (apparent N)/N ratio in Michaelis–Menten plots and Scatchard plots, respectively, are given for the various values of kn, KN and α. The note in the last part of the Table 2 legend, related to the use of Eqs. (15) and (14) (U^b) or Eqs. (23) (B_S^b) and (14) instead of Eqs. (15) and (16), still applies for the X_o/N and X_r/N ratio values in the Table.

2.2.3. *Modulation by K, N and kn of the effect of α neglect*

For given values of α, β, γ and kn (involving $\alpha = 0.75$) and various values of KN involving either a constant N value and increasing K values ($1/N$, $10/N$ and $100/N$) or a constant K value and increasing N values ($10/K$, $30/K$ and $100/K$), Figs. 4 and 5 show the Scatchard graphs obtained. The curvature of the hyperbola segment (which looks like a straight line segment for $KN = 1$, as shown in Fig. 4) becomes more pronounced with increasing values of KN. Moreover, when KN is very high relative to ϕ, Y_o and S_o are close to their upper limits, $\psi/(1-\alpha)\,(< (\alpha(kn+1))/(1-\alpha))$ and $\phi/((1-\alpha)N)\,(< (kn+1)/((1-\alpha)N))$, respectively (Fig. 4). The former ex-

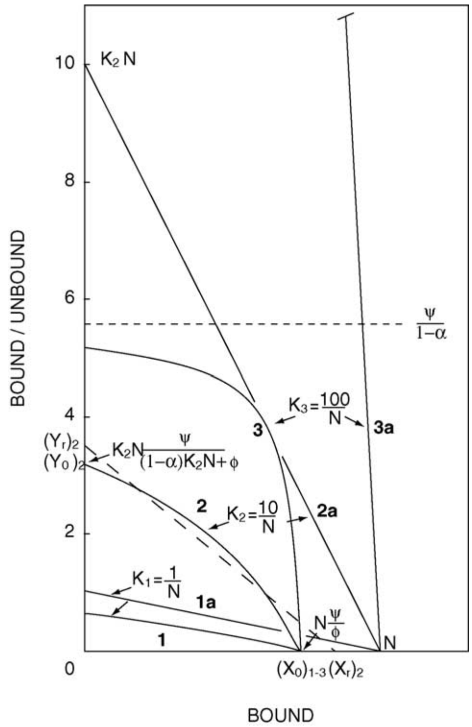

Fig. 4. Scatchard graph of specific binding when the method parameter α is not taken into account-effect of K. Equilateral hyperbola segments **1**, **2**, and **3** represent Scatchard plots for a simple R/L interaction, resulting from the use of Eqs. (15) and (16) which afford B_S^a and U^c, an underestimate of B_S and an overestimate of U, respectively. These curves are related to $\alpha = 0.75$, $\beta = 0.1$, $\gamma = 0.01$, $kn = 1$, an undetermined but constant value of N and increasing values of K, such as: $K_1 = 1/N$ (curve **1**), $K_2 = 10/N$ (curve **2**) and $K_3 = 100/N$ (curve **3**). For comparison, corresponding straight line segments **1a**, **2a** and **3a** are shown, which are obtained when exact expressions of B_S (Eq. (9)) and U (Eq. (10)) are used. Values attributed to α, β, γ and kn parameters define a hyperbola family (whose members are specified by the various values of KN). Curve intercepts are only specified for **2**, $((X_o)_{1-3} = N(\psi/\phi)$ and $(Y_o)_2 = K_2N(\psi/((1-\alpha)K_2N+\phi))$, where $\psi = (\alpha-\beta)kn + \alpha - \gamma$ and $\phi = (1-\beta)kn + 1 - \gamma$). The horizontal half straight line at $\psi/(1-\alpha)$ ordinate (short dashed line) marks the upper limit of the hyperbola family area; this horizontal line (whose position is independent of KN) constitutes the limit for the tangent to hyperbola at the intercept on the ordinate axis when KN becomes very high. From each hyperbola, apparent N and apparent K could be deduced from a set of hyperbola points. This is illustrated for curve **2**; 10 hyperbola points, i.e. five having the abscissae $0.2(X_o)_{1-3}$, $0.4(X_o)_{1-3}$, ..., $(X_o)_{1-3}$, and five having the ordinates $0.2(Y_o)_2$, $0.4(Y_o)_2$, ..., $(Y_o)_2$, were used to determine a least-squares straight regression line (long dashed line, correlation coefficient, $r = 0.97$). Apparent N and apparent KN are then defined by intercepts ($(X_r)_2 = 0.844$ N and $(Y_r)_2 = 3.53$) of this regression line on abscissa and ordinate axes; apparent K is then $(S_r)_2 = (Y_r)_2/(X_r)_2 = 0.418\,K_2$. With values attributed to α, β, γ and kn parameters, hyperbola segments **1**, **2** and **3** fit with any value of N and K provided that $K_1N = 1$, $K_2N = 10$ and $K_3N = 100$.

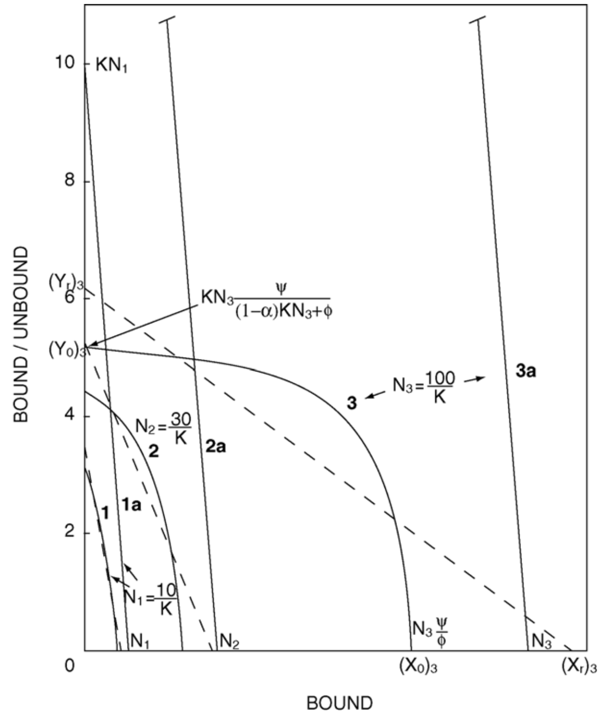

Fig. 5. Scatchard graph of specific binding when the method parameter α is not taken into account-effect of N. Equilateral hyperbola segments **1**, **2** and **3** represent Scatchard plots for a simple R/L interaction, resulting from the use of Eqs. (15) and (16) which give B_S^a and U^c, an underestimate of B_S and an overestimate of U, respectively. These curves are related to $\alpha = 0.75$, $\beta = 0.1$, $\gamma = 0.01$, $kn = 1$, an undetermined but constant value of K and increasing values of N, such as: $N_1 = 10/K$ (curve **1**), $N_2 = 30/K$ (curve **2**) and $N_3 = 100/K$ (curve **3**). For comparison, corresponding straight line segments **1a**, **2a** and **3a** are shown, which are obtained when exact expressions of B_S (Eq. (9)) and U (Eq. (10)) are used. Curve intercepts are only specified for **3**, $((X_o)_3 = N_3(\psi/\phi)$ and $(Y_o)_3 = KN_3(\psi/((1-\alpha)KN_3+\phi))$, where $\psi = (\alpha-\beta)kn + \alpha - \gamma$ and $\phi = (1-\beta)kn + 1 - \gamma$). Least-squares regression lines (dashed lines), established as described in the Fig. 4, are shown for curves **1** (correlation coefficient, $r = 0.97$), **2** ($r = 0.90$), and **3** ($r = 0.80$). Apparent N, i.e. $(X_r)_3$, and apparent KN, i.e. $(Y_r)_3$, are only specified for curve **3**. (apparent N)/N and (apparent K)/K ratios (where apparent $K = S_r = Y_r/X_r$) calculated from the intercepts of regression lines on abscissa and ordinate axes, are 0.844 and 0.418 for **1**; 0.954 and 0.182 for **2**; 1.10 and 0.0562 for **3**. With values attributed to α, β, γ and kn parameters, hyperbola segments **1**, **2** and **3** fit with any value of N and K provided that $KN_1 = 10$, $KN_2 = 30$, and $KN_3 = 100$.

pression is independent of KN, whereas the second expression is independent of K. The former result indicates that for given values of kn, α, β and γ parameters, and irrespective of K and N, the hyperbola segment is restricted to the area defined by the vertical straight line at N abscissa and the horizontal straight line at $\psi/(1-\alpha)$ ordinate. Note that it would be theoretically possible to determine K from the right section of the hyperbola segment since the slope of the tangent to the curve at X_o is equal to K (the same consideration applies for the left section of the hyperbola obtained using the Lineweaver–Burk plot, not shown). In practice, especially when K is very high ($>10^{10}$ M^{-1}), reliable determination of the tangent would require very accurate B_S^a values for increasing R saturation levels, all of which should be very close to full saturation. This requirement is very difficult to fulfil due to the magnitude of experimental errors in the measurement of B_1 and B_2 and then in the calculation of B_S^a at high R saturation level.

The combined effect of KN and α on apparent N and apparent K determined from the Michaelis–Menten plot (i.e. X_0 and S_0) and from a regression line related to the Scatchard plot (i.e. X_r and S_r) was then assessed. For given values of

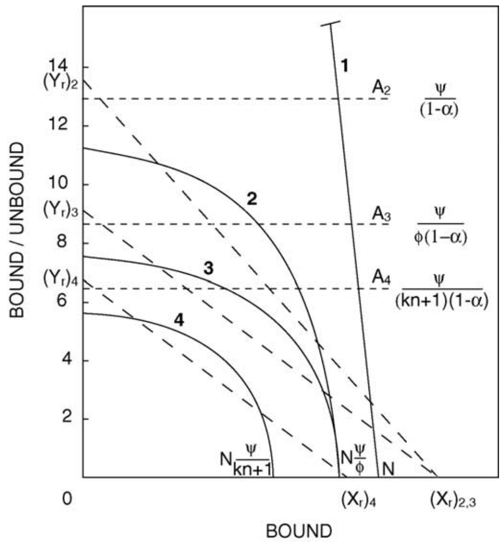

Fig. 6. Scatchard graph of specific binding according to expressions used to determine B_S and U. In the case of a simple R/L interaction characterized by $KN = 100$, a L nonspecific binding, whose coefficient is $kn = 1$, and a separation method characterized by parameters $\alpha = 0.9$, $\beta = 0.5$ and $\gamma = 0.01$, curves **1** to **4** illustrate Scatchard plots, related to the R/L interaction, which are obtained according to the expressions used to calculate B_S and U. Regular straight line segment **1**, independent of kn, α, β and γ is obtained when Eqs. (9) and (10), which afford exact B_S and U values, are used. When α has not been determined and kn has or has not been determined, various eqns which give approximate values of B_S and/or U could be used. Equilateral hyperbola segment **2** is obtained when Eqs. (15) (B_S^a) and (16) (U^c) are used. The various characteristics ($(X_o)_2$, $(Y_o)_2$, apparent N, apparent K, upper limit area, etc.) of this hyperbola are defined in the Figs. 3–5 and Tables 1–4 legends. Equilateral hyperbola segment **3** is related to the use of Eqs. (15) and (14) (U^b) and hyperbola **4** to the use of Eqs. (23) (B_S^b) and (14). Hyperbola **3** derives from **2** by affine transformation (applied from the abscissa axis, transformation coefficient $1/\phi$, where $\phi = (1-\beta)kn + 1 - \gamma$). Then curve **3** affords $(X_o)_3 = (X_o)_2 = N(\psi/\phi)$ (where $\psi = (\alpha - \beta)kn + \alpha - \gamma$) and $(Y_o)_3 = KN(\psi/(\phi[(1-\alpha)KN + \phi]))$ (instead of $(Y_o)_2 = KN(\psi/((1-\alpha)KN + \phi))$ for hyperbola **2** family). Hyperbola **4** derives from **3** by homothety (applied from the axis origin, coefficient $\phi/(kn+1)$). Consequently, (i) curve **4** affords $(X_o)_4 = N(\psi/(kn+1))$ and $(Y_o)_4 = KN(\psi/((kn+1)[(1-\alpha)KN + \phi]))$, and (ii) straight lines defined by intercepts of **3** and **4** on axes are parallel (slope, $K(1/((1-\alpha)KN + \phi))$); this is also the case for tangents to the two curves at the abscissa intercept (slope $K(1/\phi)$). Upper limits of hyperbolae **3** and **4** families are materialized by half-horizontal straight lines A_3 and A_4 at $\psi/(\phi(1-\alpha))$ and $\psi/((kn+1)(1-\alpha))$ ordinates, respectively (instead of $\psi/(1-\alpha)$ materialized by A_2 for hyperbola **2** family). Apparent N_s ($(X_r)_{2,3}$ and $(X_r)_4$) and apparent KNs ($(Y_r)_2$, $(Y_r)_3$ and $(Y_r)_4$), defined on axes by least-squares regression lines (long dashed lines), are shown for the three hyperbola segments. They were established from twenty hyperbola points, with ten having the abscissae $0.1X_o$, $0.2X_o$, ..., X_o and ten having the ordinates $0.1Y_o$, $0.2Y_o$, ..., Y_o. Calculated (apparent N)/N ratios (X_r/N) are 1.20 for **2** and **3**, and 0.90 for **4**, whereas calculated (apparent K)/K ratios (where apparent $K = Y_r/X_r$) are 0.113 for **2**, and 0.0759 for **3** and **4**; the common correlation coefficient for the three lines is $r = 0.87$. With values attributed to α, β, γ and kn parameters, hyperbola segments **2**, **3** and **4** fit with any value of N provided that $KN = 100$.

kn, β and γ ($kn = 1$, $\beta = 0.1$ and $\gamma = 0.01$, the two latter values reflecting the use of a selective separation method) and for various α and KN pairs of values, Tables 1 and 2 show the calculated values of S_o/K and S_r/K ratios and those of X_o/N and X_r/N ratios, respectively. Both S_o/K and S_r/K ($S_r \leq S_o$) increase when α increases and decrease when KN increases. For $KN \leq 1$, irrespective of the α value, the two practically identical ratios are close to 1. In contrast for $KN \geq 10$, regardless of the α value, the two ratios (differing by a factor < 1.5) are much lower, and the ratios decrease as α decreases or KN increases and become very low, e.g. close to 0.02 for $\alpha = 0.25$, $KN = 100$ or $\alpha = 0.9$, $KN = 1000$. In sharp contrast with the variations in S_o/K and S_r/K, those in X_o/N and X_r/N, according to α and KN, are considerably smaller. The X_o/N ratio (independent from KN) remains very close to the α value, whereas the X_r/N ratio ($X_r \geq X_o$) increases with increasing α or increasing KN. For $KN \leq 1$, X_r/N is very close to X_o/N and to α. It becomes > 1 when $\alpha \geq 0.75$ and $KN \geq 100$, but remains < 1.5 even for high KN (as high as 1000) and α (as high as 0.9) values. The results shown in Table 1 indicate that, especially for a high affinity R/L interaction, the apparent K determined by R saturation analysis decreases as the R concentration increases. This is illustrated in Fig. 5 (involving $\alpha = 0.75$) with three different concentrations of R, N_1, N_2, and N_3, proportional to 1, 3 and 10, respectively, such as $KN_1 = 10$. In all three cases, calculated X_0 (0.74 N) and X_r are close to N, whereas 3- and 10-fold increases in the R concentration result in 2.1-fold and 6.1-fold decreases in S_0 and 2.3-fold and 7.4 fold decreases in S_r.

The influence of the kn parameter value combined with that of α and that of KN was determined. Tables 3 and 4 show the S_o/K and S_r/K ratios and the X_o/N and X_r/N ratios, respectively, calculated for three α values and two KN values when kn ranges from 0.1 to 10 (using $\beta = 0.1$ and $\gamma = 0.01$). For $KN = 1$ and for the various α and kn pairs of values, the, practically identical, S_o/K and S_r/K ratios are close to the α value; they slightly increase (<1.5-fold) when kn ranges from 0.1 to 10. For $KN = 100$, the still close (less than two-fold difference) S_o/K and S_r/K ratios markedly increase with increasing kn, e.g. starting from very low values: 0.01–0.07, the S_r/K ratio increases 12-, 10- and 7-fold for $\alpha = 0.5$, 0.75 and 0.9, respectively, when kn increases from 0.1 to 10 (Table 3). The X_o/N ratio does not markedly vary, according to kn, it remains very close to the α value. The X_r/N ratio is close to the α value for $KN = 1$. For $KN = 100$, this ratio varies slightly according to kn, with in all cases $0.6 < X_r/N < 1.4$ (Table 4). These results (related to low β and γ values) indicate that at high KN, the kn value weakly affects the apparent N, but could markedly modulate the KN-induced decrease in apparent K.

As β and γ parameters should usually be small relative to 1 (due to dissociation of most nonspecific binding and efficient removal of unbound L when running the separation method), the effects on apparent N and K resulting from variations in these two parameters were not thoroughly studied, however simulations made with $\beta = 0.5$ instead of 0.1, using various α values (from 0.5 to 0.9) and KN values (from 0.01 to 1000) indicated that this marked increase in the β value mainly resulted in little decrease (<2.3-fold) in apparent N (X_o or X_r) irrespective of α and KN, whereas apparent K (S_o or S_r) was practically unchanged for $KN \leq 1$ and at most ∼1.3-fold decreased for $KN = 100$ or 1000 (not shown).

All these results suggest that, depending mainly on the KN value and to a lesser extent on α and kn values, considerable underestimation of K could result from the R saturation analysis approach when $\alpha \neq 1$ is not taken into account.

2.2.4. Effect of α and kn neglect

When neither α nor kn have been determined, Eqs. (14) and (15), which only involve B_1, B_2 and T, could be used to calculate U^b and B_S^a. Since $U^b/U^c = \phi$ (cf. Appendix), the equation relating B_S^a/U^b to B_S^a, established from Eq. (19), is:

$$\frac{B_S^a}{U^b} = \frac{\psi}{\phi} \times \frac{K(\psi N - \phi B_S^a)}{(1-\alpha)K(\psi N - \phi B_S^a) + \phi\psi}. \tag{22}$$

The representation of $B_S^a/U^b = f(B_S^a)$ leads to a portion of equilateral hyperbola, which derives from the previous hyperbola (related to $B_S^a/U^c = f(B_S^a)$ by an affine transformation applied from the abscissa axis, with coefficient $1/\phi$ (Fig. 6). Consequently, the intercept of the curve on the abscissa axis is still $X_o = N(\psi/\phi)$, whereas its intercept on the ordinate axis is $Y_o = KN(\psi/(\phi[(1-\alpha)KN + \phi]))$.The slope of the straight line defined by hyperbola intercepts, $S_o = K/((1-\alpha)KN + \phi)$, and that of the tangent to the curve at X_o, K/ϕ, as well as that of the regression line homologous to that of the previous hyperbola are ϕ-fold lower than those of the previous hyperbola. This, however, does not change X_r. Therefore the values of X_o/N and X_r/N ratios in Table 2 still apply for this second hyperbola family, whereas the values of S_o/K and S_r/K ratios in Table 1 should be divided by ϕ (i.e. 1.89 with values attributed to kn, β and γ) to apply to the new hyperbola family. It is noteworthy that the latter ratios are still decreasing functions of KN and increasing functions of α. However, in sharp contrast with the previous situation, they are decreasing functions of ϕ or kn.

In most binding studies B_S is assimilated to:

$$B_S^b = (B_1 - B_2) \tag{23}$$

since

$$\frac{B_S^a}{B_S^b} = \frac{T}{T - B_2} = \frac{kn+1}{\phi} \tag{24}$$

the equation relating B_S^b/U^b to B_S^b could be obtained by changing B_S^a to $B_S^b((kn+1)/\phi)$ in Eq. (22):

$$\frac{B_S^b}{U^b} = \frac{\psi}{kn+1} \times \frac{K[\psi N - (kn+1)B_S^b]}{(1-\alpha)K[\psi N - (kn+1)B_S^b] + \phi\psi}. \tag{25}$$

The curve representing $B_S^b/U^b = f(B_S^b)$ derives from hyperbola representing $B_S^a/U^b = f(B_S^a)$, by a homothety applied from the axis origin, with coefficient $\phi/(kn+1)$ (Fig. 6). The curve intercepts on axes are $X_o = N(\psi/(kn+1))$ and $Y_o = KN(\psi/((kn+1)[(1-\alpha)KN + \phi]))$, respectively. As for the second hyperbola family, the slope of the straight line defined by the hyperbola intercepts on axes and that of the tangent to the curve at the abscissa intercept are $S_o = K/((1-\alpha)KN + \phi)$ and K/ϕ, respectively. Then values of S_o/K and S_r/K in Table 1 and those of X_o/N and X_r/N in Table 2 related to the first hyperbola family, should be divided by ϕ (i.e. 1.89, with the values attributed to kn, β and γ) and by $(kn+1)/\phi$ (i.e. 1.0582), respectively, to account for the ratios related to the third hyperbola family. Therefore the use of B_S^b and U^b, instead of B_S^a and U^c, has different effects on the kn modulation of apparent K and apparent N, with little effect on apparent N and a marked decrease in apparent K at high kn (not shown).

3. Discussion

This investigation, is related to a simple R/L interaction (with equivalent and noncooperative binding sites) in the presence of nonspecific (linear) L binding. The results indicate that reliable determination of binding parameters N and K by saturation analysis experiments, involving a process to separate bound and unbound L, should require prior determination of the nonspecific binding parameter kn and especially that of the separation method parameter α. The consequences of kn or α (<1) neglect on the N and the K determinations are very dissimilar. When α but not kn has been determined, the use of appropriate expressions to calculate bound (B_S) and unbound (U^a) L concentrations does not change the type (linear or hyperbolic) of regular plots and the latter afford correct N and underestimation of K by factor $(kn+1)$. When α ($\alpha \neq 1$) has not been determined, the type of theoretical binding isotherms is changed (i.e. an equilateral hyperbola segment is obtained using the Scatchard plot, whereas non-equilateral hyperbola portions are obtained using the Michaelis–Menten plot and the Lineweaver–Burk plot) and the curves lead to apparent N and apparent K, which are lower than N and K. The values of the various binding (K, N and kn) and method (α, β, γ) parameters and the expressions used to calculate specifically bound (B_S^a or B_S^b) and unbound (U^a, U^b or U^c) L concentrations determine the magnitudes of N and K underestimations. In the common situation where β and γ are relatively low (reflecting the use of a selective separation method) only four parameters (α, K, N and kn) have important but differing impacts on the magnitudes of N and K underestimations. Apparent N (X_0, independent of KN, or X_r) is roughly equal to αN; then the N underestimation is usually moderate. In contrast, the magnitude of potential K underestimation is primarily determined by the KN value with, regardless of the α and kn values, little underestimation when $KN < 1$, and an underestimation which could be considerable for high KN values. In the latter case, in addition to α, kn modulates the magnitude of K underestimation. Obviously, as shown in Fig. 6 the various expressions used to calculate approximate values of B_S and U affect N and K underestimations differently. In order to minimize such underestimations (especially the K underestimation), it is important to use the most appropriate expressions for B_S and U, i.e. expressions involving minor B_S underestimation or minor U overestimation (e.g. B_S^a better than B_S^b, and U^c better than U^b, when α has not been determined).

When $\alpha \neq 1$ is not taken into account, the K underestimation is primarily due to B_S underestimation which results in U overestimation since U (which is not directly determined) is connected to B_S via T. The use of expressions such as U^b and U^c, which overestimate U by including a significant fraction (related to $(1-\alpha)$) of B_S, results in the limitation of the apparent B_S/U ratio (Figs. 3–7). At low R saturation level instead of being close to KN, the apparent B_S/U ratio will be $< \alpha/(1-\alpha)$, a value independent of K and N. This roughly explains why the K underestimation is greater as KN increases.

Note that other artefacts not analyzed in this study, due to the presence of radiochemical impurities in L [1–4], incomplete equilibrium [4,8], the instability of unbound R [4–6], etc., could result in similar erroneous binding isotherms (i.e. the Scatchard graph accounting for the R/L interaction would consist of a convex-upward curve) and then could similarly result in B_S underestimation and/or U overestimation. In the case of high KN, as documented in this paper, for $\alpha \neq 1$, such artefacts could lead to considerable underestimation of K. Obviously, a combination of such anomalies and $\alpha < 1$, would have additive deleterious effects on the theoretical binding isotherms and the K determination in the case of high KN.

In many instances, the combined conditions of $\alpha \neq 1$ and high KN apply. This especially occurs for determinations of K related to estrogen receptor α/[^{3}H] ligand interactions. (1) When compared with equilibrium dialysis, the usual processes (charcoal absorption, ion exchange chromatography, gel filtration, etc.) run to separate receptor-bound and unbound estrogen or antiestrogen, afford B_S values clearly lower than that obtained by running equilibrium dialysis [13], indicating that $\alpha < 1$ for these separation methods. (2) As pointed out by (i) saturation analysis experiments [12] involving [^{125}I] iodoestradiol and highly diluted receptor samples (~10^{-11} M-allowed by ^{125}I specific activity), and (ii) kinetic experiments (for k_1 and k_2 determinations) [9,10] involving potent estrogens (such as estradiol) or potent antiestrogens (such as 4-hydroxytamoxifen), the K values related to these receptor/ligand interactions are in the 10^{11}–10^{12} M^{-1} range. (3) Due to ^{3}H relatively low specific activity (compared to that of ^{125}I) receptor saturation experiments involving [^{3}H] estrogen or [^{3}H] antiestrogen require the use of samples containing nM concentrations of receptor. As a consequence of the above points (1)–(3), the latter experiments are characterized both by $\alpha < 1$ (sometimes markedly lower than 1 [12]) and $KN > 10^2$. These two characteristics alone could explain why, for potent estrogens and antiestrogens, K determined by saturation analysis of the receptor using [^{3}H] ligands is usually close to 10^9 M^{-1} [9,10], i.e. considerably underestimated. Obviously, as previously mentioned, other artefacts, e.g. resulting from radiochemical impurities in the [^{3}H] ligand source, could contribute to the K underestimation.

The fact that as KN increases the K underestimation increases could explain why the apparent K related to a high affinity R/L interaction is sometimes not markedly different from that corresponding to a much lower R/L′ or R′/L interaction, e.g. (i) ligands such as tamoxifen displaying both a k_1/k_2 ratio [10] and a competitive binding efficiency [21] ~300-fold lower than those of estradiol, showed in saturation analysis experiments an apparent K only ~10-fold lower than that of estradiol [10], and (ii) the dissociation rate of estradiol from the His 524 Ala estrogen receptor α mutant was found ~250-fold higher than that from the wild-type receptor [22], whereas the estradiol apparent K for the mutant receptor was found only to be ~12-fold lower than that for the wild-type receptor [23].

As discussed above in the case of estrogen receptor/ligand interactions, $\alpha < 1$ could be common to standard separation processes. More generally the decrease in B_S could be due to the fact that, relative to R recovery, the process is not quantitative, and/or (even concerning a quantitative process) the RL complex displays moderate stability, so a fraction of the RL complexes dissociates during the separation process. High KN values ($>10^2$) could be especially obtained in the case of very high affinity R/L interactions, but also with lower affinity R/L interactions provided that the R concentrations in cell extracts are high (e.g. in the μM range, possibly resulting from R overexpression in cells, yeast or bacteria).

In most binding studies involving a separation procedure, α is not predetermined; moreover, the $(B_1 - B_2)$ expression is assumed to account for B_S. An easy way to ensure that K (related to a simple R/L interaction) determined from a pseudo-equilibrium approach is not underevaluated (resulting from $\alpha < 1$ or other artefacts such as the presence of radioactive impurities in L), is to carry out parallel experiments with two or three different dilutions of the R preparation. If experimental K proves to be independent of the R concentration, then the determined value is probably reliable, whereas if K increases as the R concentration decreases (as shown in Fig. 5), this would suggest that the conditions used for K determination are not adequate and that K is likely underestimated. In this situation, to limit K underestimation, it would be better to run experiments with the highest dilution of R, compatible with accurate binding data determinations. Checking experiments, involving R dilution, would be especially required when experimental $KN > 1$. Note that when, e.g. due to α neglect, K is underestimated, the shape of the theoretical R/L binding isotherm suggests positive cooperativity (Figs. 3–6); however, the observed increase in experimental K by R dilution would be totally incompatible with positive cooperativity of L binding.

Kinetic association and dissociation experiments and competition binding at equilibrium are alternative approaches for determining K (k_1/k_2 ratio and relative K, respectively), which are much less susceptible to K underestimation than the saturation analysis approach. The advantages and limitations of these approaches in K determination will be the focus of another investigation.

Acknowledgement

This work was supported by the “Institut National de la Santé et de la Recherche Médicale” and the “Association pour la Recherche sur le Cancer”.

Appendix

A.1. Relation between Scatchard coordinates when no distinction is made between specific binding and nonspecific binding

When no distinction is made between B_S and B_{NS} (e.g. when a single series of equilibrium dialyses, using increasing concentrations of radioactive L are performed), the Scatchard coordinates become, $X = B_S + B_{NS}$ and $Y = (B_S + B_{NS})/U$, then:

$$Y = K(N - B_S) + kn = K[N - (B_S + B_{NS})] + KB_{NS} + kn$$

hence

$$Y = K(N - X) + Kkn\,U + kn.$$

Since $X/Y = U$, the above expression could be written:

$$Y = K(N - X) + Kkn\frac{X}{Y} + kn$$

then

$$Y^2 + KYX - (KN + kn)Y - Kkn\,X = 0.$$

This equation leads to:

$$X = \frac{Y(KN + kn - Y)}{K(Y - kn)}$$

or

$$Y = \frac{K(N - X) + kn + \sqrt{[K(N - X) + kn]^2 + 4Kkn\,X}}{2}.$$

These equations apply to an hyperbola whose asymptotes are defined by $Y = K(N - X)$ and $Y = kn$, respectively.

A.2. Relations between Michaelis–Menten, Scatchard or Lineweaver–Burk coordinates when equations with approximate B_S and U values are used

When α and/or kn have not been determined, Eqs. (9) and (10) cannot be used. Related equations, mainly obtained by neglecting α, kn or both, could be used. The equations involving underestimates of B_S or overestimates of U are:

$$B_S^a = (B_1 - B_2)\frac{T}{T - B_2} \quad (15),$$

(B_S underestimation factor, $(T - B_2)/(\alpha T - B_2) = \phi/\psi$),

$$B_S^b = (B_1 - B_2) \quad (23),$$

(B_S underestimation factor, $T/(\alpha T - B_2) = (kn + 1)/\psi$),

$$U^a = \frac{\alpha T - B_1}{\alpha T - B_2}T = T - B_S = (kn + 1)U \quad (11),$$

(U overestimation factor, $(kn + 1)$),

$$U^c = \frac{T - B_1}{T - B_2} \times \frac{T}{kn + 1} = \frac{T - B_S^a}{kn + 1} \quad (16),$$

(U overestimation factor, $(\psi(T - B_1))/(\phi(\alpha T - B_1)) > 1$),

$$U^b = T - B_1 = \phi U^c \quad (14),$$

$$U^d = T - B_S^a = (kn + 1)U^c \quad (17),$$

where $\phi = (1 - \beta)kn + 1 - \gamma$, and $\psi = (\alpha - \beta)kn + \alpha - \gamma$.

Note that provided $\gamma < (1 - \beta)kn$, a condition that practically always applies, $U^d > U^b > U^c > U$.

Depending on whether α and/or kn have or have not been determined, equations which lead to minor underestimation of B_S and minor overestimation of U should be used in order to minimize error in N and K determination. Three situations could occur:

A.2.1. α determined, kn not determined

In this case, Eqs. (9) and (11) which determine B_S and U^a, an overestimate by factor $(kn + 1)$ of U should be used. When $\alpha < 1$ the use of U^b instead of U^a ($\gamma < (1 - \beta)kn$ implies that $U^b > U^a$) will have very unfavourable consequences on the determination of N and K. This can be observed, for instance, through the Scatchard plot. From Eq. (14), U^b could be written:

$$U^b = [B_S + (kn + 1)U] - [\alpha B_S + (\beta\,kn + \gamma)U]$$

therefore,

$$U^b = (1 - \alpha)B_S + \phi U$$

and

$$\frac{U}{U^b} = \frac{1}{(1 - \alpha)(B_S/U) + \phi}.$$

Since

$$\frac{B_S}{U^b} = \frac{B_S}{U}\frac{U}{U^b}$$

and

$$\frac{B_S}{U} = K(N - B_S)$$

hence

$$\frac{B_S}{U^b} = \frac{K(N - B_S)}{(1 - \alpha)K(N - B_S) + \phi}.$$

The Scatchard plot of $B_S/U^b = f(B_S)$ would then involve an equilateral hyperbola segment, instead of the straight line segment obtained for the plot of $B_S/U^a = f(B_S)$. The hyperbola segment is convex-upward and its intercepts on abscissa and ordinate axes are $X_o = N$ and $Y_o = KN(1/((1 - \alpha)KN + \phi))$, respectively; the slope of the straight line defined by these two intercepts is $S_o = K(1/((1-\alpha)KN+\phi))$; then the S_o/K ratio is an increasing function of α and a decreasing function of KN and ϕ (or kn).

Note that when $\alpha = 1$, $B^a_S = B_S$, then the use of Eqs. (15) and (14) or Eqs. (23) and (14), would afford a linear Scatchard plot, whose intercepts on abscissa and ordinate axes are N and $KN(1/\phi)$ or $N(\phi/(kn+1))$ and $KN(1/(kn+1))$, respectively, therefore in both cases apparent K would be K/ϕ

A.2.2. kn determined, α not determined

In this case, Eqs. (15) and (16) which result from neglect of α in Eqs. (9) and (10), respectively, should be used. As previously mentioned:

$$\frac{B^a_S}{B_S} = \frac{\psi}{\phi} \text{ and } \frac{U^c}{U} = \frac{\psi}{\phi} \times \frac{T-B_1}{\alpha T - B_1}.$$

Since

$$T - B_1 = (1-\alpha)B_S + \phi U$$

and

$$\alpha T - B_1 = \psi U$$

then

$$\frac{U^c}{U} = \frac{\psi}{\phi} \times \frac{(1-\alpha)B_S + \phi U}{\psi U} = \frac{1-\alpha}{\phi} \times \frac{B_S}{U} + 1.$$

B^a_S/U^c can be written:

$$\frac{B^a_S}{U^c} = \frac{B^a_S}{B_S} \times \frac{B_S}{U} \times \frac{U}{U^c}.$$

Since

$$\frac{B_S}{U} = K(N - B_S) = K\left(N - \frac{\phi}{\psi}B^a_S\right)$$

then

$$\frac{B^a_S}{U^c} = \frac{\psi}{\phi}K\left(N - \frac{\phi}{\psi}B^a_S\right)\frac{1}{((1-\alpha)/\phi)K(N-(\phi/\psi)B^a_S)+1}.$$

The latter equation can be rewritten:

$$\frac{B^a_S}{U^c} = \frac{\psi K(\psi N - \phi B^a_S)}{(1-\alpha)K(\psi N - \phi B^a_S) + \phi\psi} \quad (19).$$

Eq. (19) applies to an equilateral hyperbola whose asymptotes are defined by:

$$X = N\frac{\psi}{\phi} + \frac{\psi}{(1-\alpha)K}$$

and

$$Y = \frac{\psi}{1-\alpha}.$$

The derived function of (19) is:

$$-K(\phi\psi)^2/[(1-\alpha)K(\psi N - \phi B^a_S) + \phi\psi]^2.$$

Then regardless of α, β, γ, K, N and kn values, the hyperbola segment is convex-upward. The slopes of tangents to the hyperbola at intercepts on the abscissa and ordinate axes are K and $K[\phi/((1-\alpha)KN+\phi)]^2$, respectively.

Considering the Michaelis–Menten plot, Eq. (19) could be used to establish the relation between corresponding Michaelis–Menten coordinates ($X = U^c$ and $Y = B^a_S$). Eq. (19) affords:

$$[\phi(1-\alpha)K]Y^2 - [\phi\psi K]YX - [\psi(1-\alpha)KN + \phi\psi]Y + [\psi^2 KN]X = 0.$$

The latter equation applies to a hyperbola whose Y asymptotic limit is $N(\psi/\phi)$ when $X \to \infty$. The slope of the tangent to the curve (convex-upward) at the origin (slope corresponding to apparent KN), calculated from the derived function of the above second degree equation (not shown), is $KN(\psi/((1-\alpha)KN+\phi))$; apparent K is then $K(\phi/((1-\alpha)KN+\phi))$. Note that contrary to the $B_S = f(U)$ representation which gives $U = 1/K$, for $B_S = N/2$, the $B^a_S = f(U^c)$ representation gives $U^c = ((1-\alpha)KN+2\phi)/(2K\phi)$ (and not $U^c = ((1-\alpha)KN+\phi)/(K\phi)$), for $B^a_S = N(\psi/(2\phi))$.

Considering the Lineweaver–Burk plot, Eq. (19) could still be used to establish the relation between the corresponding double reciprocal coordinates ($X = 1/U^c$, and $Y = 1/B^a_S$). Eq. (19) gives:

$$[\psi^2 KN]Y^2 - [\psi(1-\alpha)KN + \phi\psi]YX - [\phi\psi K]Y + [\phi(1-\alpha)K]X = 0.$$

The latter equation applies to a non-equilateral hyperbola whose Y limit (corresponding to 1/(apparent N)) is $\phi/(N\psi)$ when $X \to 0$. The slope of the asymptote (stems from the axis origin) to the useful hyperbola portion (slope corresponding to 1/(apparent KN)) is $((1-\alpha)KN+\phi)/(\psi KN)$ Apparent N and apparent K are then $N(\psi/\phi)$ and $K(\phi/((1-\alpha)KN+\phi))$, respectively. Note that the slope of the tangent to the curve (convex-downward) at the ordinate intercept, calculated from the derived function of the above second degree equation (not shown), is $\phi/(KN\psi)$; the intercept of this tangent on the ordinate axis is then at $-K$ (not shown).

A.2.3. α and kn not determined

This last situation was considered in Section 2.2.4 in the case of the Scatchard representation. Using the same approach as that described in the above section, equations and then characteristics of the Michaelis–Menten and Lineweaver–Burk curves related to the present situation could be established from Eq. (22) or (25) involving B^a_S and B^b_S, respectively.

References

[1] S.E. Builder, I.H. Segel, Equilibrium ligand binding assays using labeled substrates: nature of the errors introduced by radiochemical impurities, Anal. Biochem. 85 (1978) 413–424.

[2] E.M. Reimann, M.S. Soloff, The effect of radioactive contaminants on the estimation of binding parameters by Scatchard analysis, Biochim. Biophys. Acta. 553 (1978) 130–139.
[3] B. Honoré, Protein binding studies with radiolabeled compounds containing radiochemical impurities, Anal. Biochem. 162 (1987) 80–88.
[4] J.C. Kermode, The curvilinear Scatchard plot. Experimental artifact or receptor heterogeneity? Biochem. Pharmacol. 38 (1989) 2053–2060.
[5] G.C. Chamness, W.L. McGuire, Scatchard plots: common errors in correction and interpretation, Steroids 26 (1975) 538–542.
[6] J.S. Beck, H.J. Goren, Simulation of association curves and 'Scatchard' plots of binding reactions where ligand and receptor are degraded or internalized, J. Recep. Res. 3 (1983) 745–772.
[7] S. Swillens, J.E. Dumont, A pitfall in the interpretation of data on ligand–protein interaction, Biochem. J. 149 (1975) 779–782.
[8] J.M. Boeynaems, J.E. Dumont, Quantitative analysis of the binding of ligands to their receptors, J. Cyclic Nucleotide Res. 1 (1975) 123–142.
[9] H. Truong, E.E. Baulieu, Interaction of uterus cytosol receptor with estradiol. Equilibrium and kinetic studies, Biochim. Biophys. Acta. 237 (1971) 167–172.
[10] J.L. Borgna, H. Rochefort, High-affinity binding to the estrogen receptor of [^{3}H]4-hydroxytamoxifen, an active antiestrogen metabolite, Mol. Cell. Endocrinol. 20 (1980) 71–85.
[11] A.C. Notides, N. Lerner, D.E. Hamilton, Positive cooperativity of the estrogen receptor, Proc. Natl. Acad. Sci. USA 78 (1981) 4926–4930.
[12] M. Salomonsson, B. Carlsson, J. Häggblad, Equilibrium hormone binding to human estrogen receptors in highly diluted cell extract is non-cooperative and has a K_d of approximately 10 pM, J. Steroid Biochem. Mol. Biol. 50 (1994) 313–318.
[13] G. Barbanel, J.L. Borgna, J.C. Bonnafous, J.C. Mani, Development of a microassay for estradiol receptors, Eur. J. Biochem. 80 (1977) 411–423.
[14] D. Rodbard, Mathematics of hormone-receptor interaction I. basic principles, in: B.W. O'Malley, A.R. Means (Eds.), Receptors for Reproductive Hormones, Plenum, New York, 1973, pp. 289–326.
[15] D. Rodbard, H.A. Feldman, Theory of protein–ligand interaction, in: B.W. O'Malley, J.G. Hardman (Eds.), Methods in Enzymology, vol. 36A, Academic Press, New York/London, 1975, pp. 3–16.
[16] J.P. Blondeau, P. Robel, Determination of protein–ligand binding constants at equilibrium in biological samples, Eur. J. Biochem. 55 (1975) 375–384.
[17] K.E. Mickelson, P.H. Petra, A filter assay for the sex steroid binding protein (SBP) of human serum, FEBS Lett. 44 (1974) 34–38.
[18] J.D. Baxter, D.V. Santi, G.G. Rousseau, A filter technique for measurement of steroid-receptor binding, in: B.W. O'Malley, J.G. Hardman (Eds.), Methods in Enzymology, vol. 36A, Academic Press, New York/London, 1975, pp. 234–239.
[19] A.L. Rosner, G.H. Teman, C.L. Bray, N.A. Burstein, Batch assay method evaluation of cytoplasmic estrogen receptor. Relative immunity of hydroxylapatite method from errors of measurements, Eur. J. Cancer 16 (1980) 1495–1502.
[20] G. Leclercq, Technical pitfalls, methodological improvements and quality control of steroid hormone receptor assays, Eur. J. Cancer Clin. Oncol. 23 (1985) 453–458.
[21] H. Rochefort, M. Garcia, J.L. Borgna, Absence of correlation between antiestrogenic activity and binding affinity for the estrogen receptor, Biochem. Biophys. Res. Commun. 88 (1979) 351–357.
[22] S. Aliau, H. Mattras, E. Richard, J.C. Bonnafous, J.L. Borgna, Differential interactions of estrogens and antiestrogens at the 17β-hydroxyl or counterpart hydroxyl with histidine 524 of the human estrogen receptor α, Biochemistry 41 (2002) 7979–7988.
[23] K. Ekena, K.E. Weis, J.A. Katzenellenbogen, B.S. Katzenellenbogen, Identification of amino acids in the hormone binding domain of the human estrogen receptor important in estrogen binding, J. Biol. Chem. 271 (1996) 20053–20059.